JGR Oceans

RESEARCH ARTICLE
10.1029/2020JC016874

Reconciling Between Optical and Biological Determinants of the Euphotic Zone Depth

Jinghui Wu[1,3], Zhongping Lee[2], Yuyuan Xie[1,5], Joaquim Goes[3], Shaoling Shang[1], John F. Marra[4], Gong Lin[1], Lei Yang[1], and Bangqin Huang[1]

[1]State Key Laboratory of Marine Environmental Science, College of Ocean and Earth Sciences, Xiamen University, Xiamen, China, [2]School for the Environment, University of Massachusetts Boston, Boston, MA, USA, [3]Lamont Doherty Earth Observatory at Columbia University, Palisades, NY, USA, [4]Department of Earth and Environmental Sciences, Brooklyn College, Brooklyn, NY, USA, [5]Current Addresses: NOAA, Northeast Fisheries Science Center, Milford Laboratory, Milford, CT, USA

Key Points:

- The "euphotic zone" depth based on 1% or 0.1% surface photosynthetically available radiation (PAR) is not an accurate measure of the biological euphotic zone determined on the basis of photosynthetic rate measurements
- The compensation irradiance varies significantly and thus is not an operationally useful metric to define the base of the euphotic zone
- For low-to mid-latitude waters, depths of 0.5% of surface PAR, or 0.9% of surface usable solar radiation, or 1.5% of surface downwelling irradiance at 490 nm related better with the euphotic zone depth determined biologically

Supporting Information:

Supporting Information may be found in the online version of this article.

Correspondence to:

Z. Lee and J. Wu,
Zhongping.Lee@umb.edu;
jinghuiwu1994@stu.xmu.edu.cn

Citation:

Wu, J., Lee, Z., Xie, Y., Goes, J., Shang, S., Marra, J. F., et al. (2021). Reconciling between optical and biological determinants of the euphotic zone depth. *Journal of Geophysical Research: Oceans*, *126*, e2020JC016874. https://doi.org/10.1029/2020JC016874

Received 9 OCT 2020
Accepted 10 APR 2021

Abstract

The conventional use of optically determined 1% of surface photosynthetically available radiation (PAR) depth ($Z_{1\%}^{PAR}$, λ = 400–700 nm) as a metric for the euphotic zone depth (Z_{eu}) has been a matter of debate for several decades because of frequent inconsistencies with the base of euphotic zone determined biologically, that is, the compensation depth (Z_c). In this study, we attempt to reconcile between optical and biological determinants of the euphotic zone through the use of a large data set of coincidental profiles of downwelling irradiance and primary production. These measurements cover open ocean waters in the tropics, subtropics, temperate regions, and from two time-series stations, the Hawaii Ocean Time-series (HOT) and the Bermuda Atlantic Time-series Study (BATS). We report that, at least for these measurements, $Z_{1\%}^{PAR}$ is too shallow (by 14.1%) compared to Z_c, while $Z_{0.1\%}^{PAR}$ is too deep (by 32.7%). Further, the irradiance at Z_c (i.e., the compensation irradiance, I_c) varies by a factor of more than five, but its ratio to surface irradiance is relatively stable. In general, I_c corresponds to 0.48 ± 0.23% of surface PAR, or 0.87 ± 0.40% of surface usable solar radiation (USR, for λ = 400–560 nm), or 1.50 ± 0.67% of surface downwelling irradiance at 490 nm. These results suggest that $Z_{0.5\%}^{PAR}$, or $Z_{0.9\%}^{USR}$, or $Z_{1.5\%}^{490}$ could be promising alternatives to bridge the optical and biological determinants of the euphotic zone depths for waters in the open ocean at low to middle latitudes.

Plain Language Summary

Euphotic zone depth (Z_{eu}) is an important and classical concept in biological oceanography, which serves as a useful measure of the layer that has meaningful photosynthesis or primary production (PP). Due to practical difficulties in assessing Z_{eu} through measurements of PP, it has been widely done through the measurement of light intensity under the assumption that the depth of 1% PAR(0) is this Z_{eu}. However, the use of 1% PAR(0) for estimating Z_{eu} continues to be a matter of debate as this depth generally doesn't represent the biological Z_{eu} (or compensation depth, Z_c). In this study, a large data set (234 points) has been analyzed, consisting of concurrent profiles of PP and light intensity from different parts of the global oceans and different water types, excluding high-latitude regions. The results indicate that Z_c matches well with the depth 0.5% of PAR(0) ($Z_{0.5\%}^{PAR}$), or the depth of 0.9% surface usable solar radiation (USR, λ = 400–560 nm) ($Z_{0.9\%}^{USR}$), or the depth of 1.5% of surface downwelling irradiance at 490 nm ($Z_{1.5\%}^{490}$). These results suggest that $Z_{0.5\%}^{PAR}$, or $Z_{0.9\%}^{USR}$, or $Z_{1.5\%}^{490}$ can be a promising approach to bridge optically and biologically derived Z_{eu} at least for low-to mid-latitude waters.

1. Introduction

The euphotic zone constitutes the upper layer of aquatic ecosystems, where ambient light levels are sufficient to support primary production. At any depth within this layer, net primary production (NPP, mg C m^{-3} d^{-1}) rates are always greater than zero (Falkowski, 1994). The base of the euphotic zone (Z_{eu}, m) where the rate of photosynthesis equals that of autotrophic respiration, that is, NPP = 0, has been termed the compensation depth (Z_c, m) (Kirk, 1994; Ryther, 1955). Both Z_{eu} and Z_c have frequently been used in aquatic ecology as benchmarks for describing and comparing integrated phytoplankton biomass and pigment content, nutrient inventories, NPP, quotients of total water-column light utilization index, and export production processes across different water types and different aquatic ecosystems (Ducklow et al., 2001;

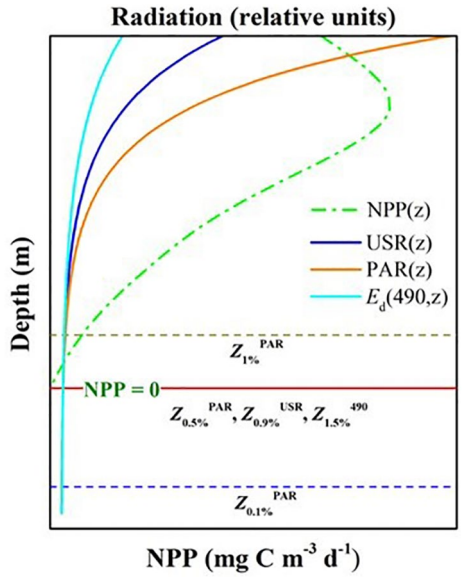

Figure 1. A conceptual figure shows the depth profiles of USR(z), PAR(z), E_d(490,z), and NPP(z), as well as the relative positions of $Z_{1\%}^{PAR}$, $Z_{0.5\%}^{PAR}$, $Z_{0.9\%}^{USR}$, $Z_{1.5\%}^{490}$, and $Z_{0.1\%}^{PAR}$. The compensation depth (NPP = 0) is the depth at which production and respiration rate are equal.

Eppley & Peterson, 1979; Richardson & Jackson, 2007). Z_{eu} in particular has often been used as a parameter for studying and understanding the interaction between photosynthesis and the ocean's carbon cycle. In oligotrophic gyres where the euphotic zone is deep, new or export production in the lower euphotic zone can be significantly more critical than that in the upper mixed layer (Letelier et al., 2004), and therefore an accurate determination of Z_{eu} is of considerable significance for biogeochemical studies in the ocean.

On account of the practical difficulties in measuring vertical profiles of NPP in the field, the determination of Z_{eu} is seldom based on Z_c, but more commonly on optical measurements. Among the earliest optical estimates of Z_{eu} were those by Steemann Nielsen (1952) and Steemann Nielsen and Hansen (1961), who suggested the use of depths corresponding to 1% of surface blue light, or 5% of surface green light. However, because solar radiation in the visible domain (400–700 nm) is the primary driver of photosynthesis, the term photosynthetically available radiation (PAR, λ = 400–700 nm) was defined (Ryther, 1956), and low-cost instruments that could easily measure PAR in air and water were developed. There have been extensive measurements of PAR profiles in the global ocean over the past decades. Since light levels at the compensation depth, that is, compensation irradiance (I_c, mol quanta m^{-2} d^{-1}), are generally about two orders of magnitude lower than the irradiance at the sea surface, the idea of utilizing the 1% light-level depth as a measure of the "euphotic zone" (Ryther, 1956) has remained popular since the 1960's (Parsons et al., 1984). This measure of the euphotic zone continues to be widely used as the "standard" to this day, in all sub-disciplines of oceanography.

Despite its widespread acceptance and extensive use by the oceanographic community, it is noteworthy that Ryther (1956) cautioned against the unrestricted use of PAR-derived Z_{eu}, indicating that it had no biological dependence other than defining the water depths below which no appreciable photosynthesis can occur. However, despite observations of frequent differences between optically derived Z_{eu} and Z_c–the desired "biological Zeu", only some studies (Banse, 2004; Laws et al., 2014; Lorenzen, 1976; Marra et al., 2014) have questioned the utility of PAR-based estimates of Z_{eu} (Z_{eu}^{PAR} or $Z_{1\%}^{PAR}$) for ecological studies. There have been attempts to use 0.1% surface PAR depth ($Z_{0.1\%}^{PAR}$) instead of $Z_{1\%}^{PAR}$ to define the euphotic zone depth (Banse, 2004; Holm-Hansen & Greg Mitchell, 1991; Hung et al., 2000), but these estimates are also arbitrary and without biological basis, with the exception of Laws et al. (2014), who used NPP profiles obtained from the Hawaii Ocean Time-series (HOT) to establish more robust relationships between optical and biological determinants of the euphotic zone depths at this site. Figure 1 shows a conceptual relationship between profiles of NPP and various light intensities. With respect to $Z_{1\%}^{PAR}$, Banse (2004) pointed out that the 1% depth of surface PAR in winter in higher latitudes could roughly be two times deeper than biologically measured Z_c, while in the tropics, $Z_{1\%}^{PAR}$ could underestimate Z_c by 50%, thus suggested the base of the euphotic zone should be based on I_c.

To demonstrate that relative measure of light intensity is still valid to estimate Z_c (or Z_{eu}) optically, Marra et al. (2014) used measurements from a cruise in the mid-latitude western North Atlantic Ocean. This work also supported the findings of Banse (2004) who showed that the Z_c was consistently deeper than the conventional $Z_{1\%}^{PAR}$ for these waters. Marra et al. (2014) also reported that the depth of 1% of surface blue light (490 nm) was superior than $Z_{1\%}^{PAR}$ as a measure of biologically derived Z_{eu}. In a separate study Laws et al. (2014) analyzed profiles of NPP and radiometric measurements obtained at HOT and concluded that 0.11% surface PAR or 1% surface blue light at 475 nm matches better with Z_c. However, studies from Marra et al. (2014) were based on 10 coincident measurements of optical and biological euphotic zone in the northwestern Atlantic Ocean in July 2008, while the study of Laws et al. (2014) was based on 16 and confined to one location or one water type.

Table 1
Cruise Details and the Number (N) of Stations With Concurrent NPP and Optical Profiles

Project	Name	Date	N	Lat (°N)	Long (°E)	Data source
CHOICE-C	The process, mechanism and its global implication of the carbon cycling in the South China Sea	July 2009 - May 2011	10	15–23	105–121	(Xie et al., 2015)
ONDEQUE	The optical and nutrient dependence of quantum efficiency	4–23 July 2008	11	32–41	−70 – −73	(Marra et al., 2014)
ASN	Quantitative importance and trophic role of *Noctiluca* blooms in the Arabian Sea	2–22 March 2008	9	17–22	66–68	https://www.bco-dmo.org/dataset/3952/data
EqPac	The Equatorial Pacific Process Study	3 Feb to 9 Mar, 5 August to18 September 1992	23	−6–12	−139 – −141	http://usjgofs.whoi.edu/jg/dir/jgofs/eqpac/
NABE	The North Atlantic Bloom Experiment	25 April to 8 June 1989	16	46–59	−17 – −20	http://usjgofs.whoi.edu/jg/dir/jgofs/nabe/
HOT	Hawaii Ocean Time-series	March 1998–October 2015	122	22° 45′	−158°00′	http://hahana.soest.hawaii.edu/hot/
BATS	Bermuda Atlantic Time-series Study	January 1992–May 2000	43	31° 45′	−64°10′	http://bats.bios.edu/

Given the widespread use of Z_{eu} and the importance of both Z_{eu} and Z_c in aquatic ecology and carbon cycling studies, it was deemed necessary and valuable to revisit the concept of euphotic zone depth by taking advantage of the extensive coincident measurements of primary production and spectral solar radiation from the different regions of the global oceans. Since our study includes datasets from a wide range of water types and from different seasons as opposed to a specific water type, it represents a significant advancement over the studies by Laws et al. (2014) and Marra et al. (2014). Our goal was to determine a more applicable optical measure of the euphotic depth that is consistent with the biological euphotic depth (Z_c). Concurrently measured biological and optical data, compiled by us, came from 69 stations spanning tropical, subtropical and temperate waters. In addition, we used 165 measurements from two time-series spanning different seasons. Variations in I_c and its relationship to irradiance at the sea surface were examined to reconcile discrepancies between biological and optical determinants of the euphotic zone. It is hoped that a better understanding of the relationships between Z_c (photosynthesis) and Z_{eu} (radiation) will offer a more insightful, convenient and useful measure of the euphotic zone depth from optical properties, at least for these low-to-middle latitude waters.

2. Data and Methods

2.1. Overall Description of the Cruises

Given the nature of this study, this data compilation effort had to be restricted to in-situ datasets that contained concurrently obtained profiles of NPP and downwelling irradiance (E_d (λ,z)), with all data either published or accessible as open source. A total of 69 sample stations from seven different cruises (detailed below) covering waters from the equator to mid-latitude waters and from two time-series fulfilled this requirement (see Table 1 and Figure 2).

(a) The CHOICE-C program, comprised of oceanographic expeditions from 2009 to 2011 in the northern South China Sea, provided 10 matched stations within 15–23°N and 105–121°E.
(b) The ONDEQUE cruise undertaken between 4 and 23 July 2008 in the western North Atlantic Ocean (32–41°N and 70–73°W) had 11 stations.
(c) The ASN cruise of 2 to 22 March 2008 which focused on *Noctiluca* blooms in the northern Arabian Sea contained 9 stations.

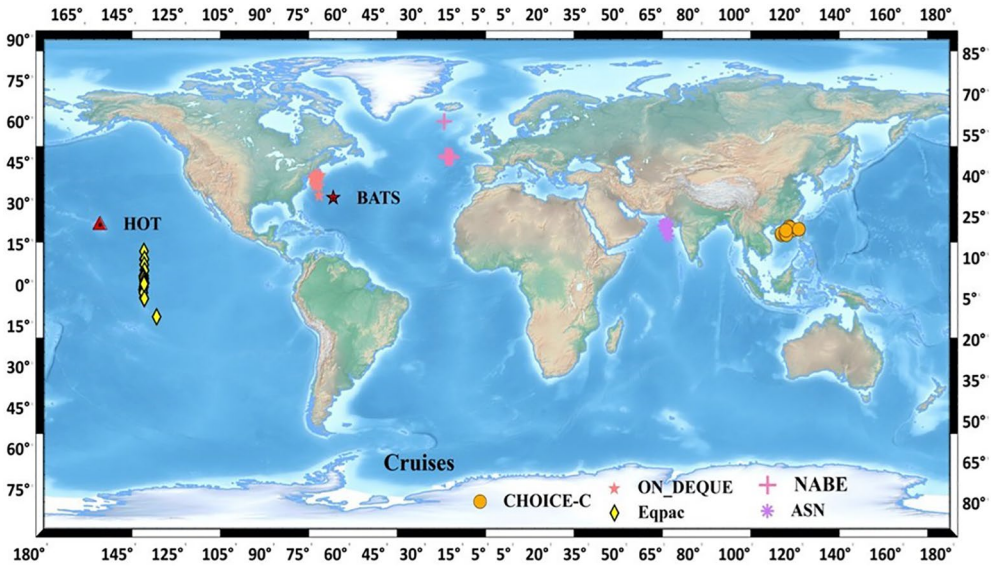

Figure 2. Location of the seven cruises, as well as the long-term oceanographic biogeochemical time-series stations (HOT and BATS) where field data are used in this study.

(d) The EqPac data set contained 23 stations located between 6°S and 12°N, around 140°W of which, 11 were obtained during spring from 3 February to 9 March, and 12 were obtained during the fall cruise from 5 August to 18 September 1992.
(e) The NABE data set contained 16 stations from two cruises in the North Atlantic Ocean (46–59°N and 17–20°W) from April 25 to June 8 in 1989.
(f) The two longest biogeochemical time-series stations, the Hawaii Ocean Time-series (HOT; 22° 45'N, 158° 00'W) in the Pacific Ocean, and the Bermuda Atlantic Time-series Study (BATS; 31° 45'N, 64° 10'W) in the North Atlantic Ocean provided 122 and 43 measurements, respectively.

The measurements were from optically and biologically diverse environments (except that no measurements in the high latitude included in this study), with highly variable chlorophyll-a concentrations (Chl, mg m^{-3}). Surface chlorophyll-a concentrations (Chl_0) varied over an extensive range of 0.01–3.11 mg m^{-3} (Table 2a). The vertical profiles of Chl also varied widely in their shape, from nearly uniform to non-uniform vertical distribution when a prominent sub-surface Chl maximum (SCM) was present. For stations with an SCM, the depth of the Chl maximum (Z_{max}, m) varied between 10 and 143 m, averaging 85 ± 29 m. Chl within the Z_{max} layer (Chl_{max}, mg m^{-3}) varied between 0.08 and 3.59 mg m^{-3}, averaging 0.42 ± 0.51 mg m^{-3}. Measurements were made under sunny and cloudy conditions, with surface PAR having a coefficient of variation (CV) of 38.9%. Surface primary production also varied significantly from 0.74 to 141.5 (13.1 ± 19.2) mg C m^{-3} d^{-1} because of the vast differences in illumination conditions and Chl. There was one exception in the ASN, where Chl and surface primary production rates were extremely high because the measurements were made during an intense *Noctiluca* bloom.

2.2. Profiles of Downwelling Irradiance

In (a) the CHOICE-C project and (c) the ASN experiment, profiles of E_d (λ,z) were obtained with an Optical Profiler II® (Satlantic, Inc., Halifax) and processed using Satlantic software (Prosoft® 7.7.10). The spectral range of the data was 350–700 nm, and the spectral interval was 10 nm. Three profiles were obtained near local noon at each station, with instruments deployed approximately 10 m away to avoid ship shadow and reflection. The final E_d (λ,z) profiles at each station are based on the average of the three profiles.

In (b) ONDEQUE, E_d (λ,z) profiles were obtained using an Optical Profiler II® (Satlantic Inc., Halifax) and provided a total of 14 channels spanning the wavelengths 380–779 nm, each with 20 nm bandwidth.

Table 2
(a) Ranges of Variables From Direct Measurements, Including I_c (after Converting Measurements of Irradiance to Units of Quanta m^{-2} s^{-1} nm^{-1}), Z_c, Chl_0, Z_{max}, and Chl_{max}. The Depths of 1% Surface PAR, USR, $E_d(490)$, and Depths of 0.1% Surface PAR Also Included. (b) Ranges of Ratios of Light Intensity, Including the Average Ratios of $I_c/PAR(0)$, $I_c/USR(0)$, $I_c/E_d(490,0)$, as well as the Ratio of $E_d(490,Z_c)$ to $E_d(490,0)$ for Each Cruise. For Each Variable, the Upper Row Represents Its Mean (±Standard Deviation) and the Lower Row Represents Its Minimum to Maximum Values

(a)

Variables	EqPac	ASN	CHOICE-C	ONDEQUE	NABE	HOT	BATS	Total
I_c (mol quanta m^{-2} d^{-1})	0.23 ± 0.08	0.29 ± 0.16	0.32 ± 0.12	0.28 ± 0.13	0.22 ± 0.15	0.17 ± 0.10	0.36 ± 0.18	0.23 ± 0.14
	0.10–0.43	0.07–0.47	0.21–0.60	0.12–0.53	0.08–0.57	0.03–0.48	0.12–0.77	0.03–0.77
PAR(0) (mol quanta m^{-2} d^{-1})	43.6 ± 8.2	68.0 ± 39.2	70.4 ± 20.5	55.6 ± 21.2	35.8 ± 19.8	39.6 ± 12.6	84.6 ± 36.8	50.6 ± 27.2
	18.9–56.1	10.7–111.7	44.9–105.5	16.3–75.9	11.7–69.7	7.4–65.2	18.1–189.3	7.4–189.6
Chl_0 (mg m^{-3})	0.20 ± 0.10	0.58 ± 0.52	0.38 ± 0.27	0.31 ± 0.19	1.39 ± 0.74	0.09 ± 0.03	0.13 ± 0.11	0.24 ± 0.41
	0.05–0.53	0.19–1.64	0.10–0.74	0.07–0.70	0.57–3.11	0.04–0.16	0.01–0.40	0.01–3.11
Chl_{max} (mg m^{-3})	0.33 ± 0.09	0.85 ± 0.45	0.70 ± 0.26	1.01 ± 0.76	1.69 ± 0.79	0.22 ± 0.04	0.20 ± 0.07	0.42 ± 0.51
	0.16–0.56	0.43–1.98	0.41–1.23	0.37–2.91	0.65–3.59	0.13–0.34	0.08–0.37	0.08–3.59
Z_c (m)	96 ± 12	57 ± 18	78 ± 15	75 ± 29	46 ± 10	130 ± 10	115 ± 12	110 ± 29
	78–118	21–80	60–93	37–137	31–67	100–157	90–135	21–157
Z_{max} (m)	78 ± 14	33 ± 15	58 ± 12	56 ± 30	27 ± 8	103 ± 16	80 ± 13	85 ± 29
	50–106	10–57	30–79	22–120	18–44	25–143	40–99	10–143
$Z_{1\%}^{PAR}$ (m)	84 ± 11	49 ± 14	66 ± 15	63 ± 24	41 ± 9	111 ± 11	96 ± 9	95 ± 24
	69–109	20–66	46–84	29–106	29–55	90–151	80–125	20–151
$Z_{0.9\%}^{USR}$ (m)	97 ± 12	58 ± 23	78 ± 16	73 ± 27	50 ± 11	125 ± 14	103 ± 9	106 ± 28
	80–124	22–83	57–100	34–125	33–68	100–170	85–124	22–170
$Z_{1\%}^{490}$ (m)	112 ± 13	66 ± 25	97 ± 25	81 ± 35	51 ± 13	140 ± 13	118 ± 13	120 ± 31
	92–141	22–97	65–125	37–158	28–69	115–174	92–163	22–174
$Z_{0.1\%}^{PAR}$ (m)	119 ± 10	95 ± 31	103 ± 21	96 ± 34	73 ± 13	161 ± 12	151 ± 11	138 ± 33
	105–140	43–133	74–126	50–158	52–98	137–175	130–173	43–175

(b)

Variables	EqPac	ASN	CHOICE-C	ONDEQUE	NABE	HOT	BATS	Total
$I_c/PAR(0)$ (%)	0.53 ± 0.16	0.45 ± 0.08	0.45 ± 0.06	0.53 ± 0.15	0.65 ± 0.26	0.44 ± 0.21	0.49 ± 0.31	0.48 ± 0.23
	0.24–0.91	0.33–0.63	0.38–0.57	0.32–0.77	0.19–1.04	0.11–1.19	0.14–1.51	0.11–1.51
$I_c/USR(0)$ (%)	0.98 ± 0.28	0.98 ± 0.20	0.95 ± 0.08	0.81 ± 0.19	1.12 ± 0.43	0.81 ± 0.39	0.85 ± 0.56	0.87 ± 0.40
	0.46–1.67	0.59–1.25	0.86–1.12	0.54–1.07	0.36–1.77	0.19–2.18	0.24–2.72	0.19–2.72
I_c/E_d (490,0) (%)	138 ± 40.0	140 ± 30.6	124 ± 30.7	121 ± 36.9	161 ± 61.8	125 ± 59.1	103 ± 73.7	125.3 ± 59.0
	69.4–230	81.2–175	78.0–173	57.3–181	53–250	28.8–336	26.7–352	26.7–352
E_d (490,Z_c)/E_d (490,0) (%)	2.04 ± 0.47	1.64 ± 0.60	1.86 ± 0.41	1.76 ± 0.52	1.47 ± 0.72	1.39 ± 0.58	1.31 ± 0.91	1.50 ± 0.67
	1.24–3.12	0.82–2.36	0.97–2.44	0.71–2.44	0.23–2.76	0.39–3.82	0.38–4.39	0.23–4.39

Data collection and processing of irradiance data in the ONDEQUE project have been detailed in Marra et al. (2014).

For (d) the EqPac and (e) the NABE projects, the instrument to measure $E_d(\lambda,z)$ and PAR profiles was a Bio-spherical Spectroradiometer (MER-1048). This MER-1048 acquires irradiance at wavelengths: 410, 441, 488, 520, 550, 560, 589, 633, 656, 671, 683, 694, and 710 nm. The profile data were commonly filtered to remove obvious data spikes and then binned into one-meter averages.

At HOT, vertical profiles of $E_d(\lambda,z)$ were obtained using a Bio-spherical PRR-600 Profiling Reflectance Radiometer (PRR) that has seven wavelength channels (412, 443, 490, 510, 555, 665 nm and PAR). The

instrument is lowered by hand and depending on the subsurface currents, is deployed to a depth between 125 and 175 meters. At BATS, $E_d(\lambda,z)$ profiles were obtained with Bio-spherical multispectral radiometers (325–665 nm).

For cruises with multispectral radiometers (e.g., MER or PRR), the multi-spectral profile of $E_d(\lambda,z)$ were first converted to hyperspectral (with a resolution of 1 nm) profiles based on Zoffoli et al. (2018). Although the units for $E_d(\lambda,z)$ or PAR do not matter when calculating the ratio of solar radiation of different depths, the measured $E_d(\lambda,z)$ were converted to mol quanta m^{-2} s^{-1} nm^{-1} by multiplying 4.6×10^{-6} (Sager & McFarlane, 1997) in order to compare these measurements with those reported in the literature. Vertical profiles of PAR(z) were then obtained by integrating $E_d(\lambda,z)$ from 400 nm to 700 nm and multiplying 1.3 to account for the difference between scalar and planar measurements of solar radiation. The resulting profiles of PAR(z) were evaluated with concurrent PAR profile measurements wherever available and were found to be consistent with each other. For all the above projects, the irradiance just beneath the water surface, $E_d(\lambda,0)$, was obtained from the intercept of the least-square exponential fits between $E_d(\lambda,z)$ and depth extending several meters below the surface (generally surface to ~7 m, depends on the sampling data), following the standardized algorithm of ProSoft 7.7 (User Manual Document: SAT-DN-00228 Copyright © 2011 by Satlantic Incorporated).

Separately, because the wavelengths most relevant for phytoplankton photosynthesis are blue-green (Dubinsky et al., 1986), which is also the spectral domain penetrating deepest in the ocean (Lee et al., 2013; Nielsen, 1952; Nielsen & Hansen, 1961), vertical profiles of usable solar radiation at time t (USR(z,t), λ = 400–560 nm) were also calculated from $E_d(\lambda,z,t)$ following Lee et al. (2014). USR basically collectively describes this photosynthetically significant radiometric energy in aquatic environment (Lee et al., 2014; Lin et al., 2016).

2.3. Profiles of Net Primary Production and Calculation of Z_c

At most stations, the vertical distribution of NPP was derived using ^{14}C-tracer methodology (Steemann Nielsen, 1952), in samples drawn from several depths in the water column, following the protocol described in the International JGOFS manual (Knap 1996). This protocol for NPP calls for the dark corrections to be made for several reasons including potential adsorption of the radioactive material onto inorganic particles apart from the non-photosynthetic uptake, which the dark correction helps eliminate. All estimates of NPP have been corrected for dark ^{14}C uptake, which are consistent with that in Marra et al. (2014) and Laws et al., (2014). Further, the determination of Z_c in our study followed that in Marra et al. (2014).

Many previous studies have estimated the Z_c from light-dark bottle O_2 incubation where the respiration is cumulatively contributed by phytoplankton, zooplankton, and bacteria. This "community Z_c" reviewed by Banse (2004) is essentially shallower than the "phytoplankton Z_c," the latter defined as the depth above which net photosynthesis is greater than 0 (Steemann Nielsen, 1952). In Ryther (1956), Z_c estimates were based on the ^{14}C uptake measurements in light and dark bottles (Steemann Nielsen, 1952) using samples drawn from different depths in the column. The depth at which ^{14}C based net photosynthesis was almost close to zero was used to define phytoplankton compensation depth (Z_c). In the study of Laws et al. (2014) they cautioned that ^{14}C fixation could also result from anaplerosis and/or chemolithoautotrophy, especially in deeper samples, and that these overestimates due to non-photosynthetic uptake of ^{14}C labeled inorganic carbon could introduce uncertainties in the estimations of Z_c. Despite its shortcomings, the ^{14}C method of Steemann Nielsen (1952) is still considered the gold standard for NPP estimates and the definition of Z_c based on this method continues to be widely used even to this day (Parsons et al., 2013). In short, for the ONDEQUE, ASN, EqPac, NABE, HOT, and BATS cruises in our study (N = 224), NPP estimates were based on the standard JGOFS protocol and used the difference between light bottle and dark bottle for obtaining dark-corrected net photosynthetic rates. More specifically,

(a) NPP estimates for the CHOICE-C cruises were based on photosynthesis-irradiance (P vs E) relationships (Platt et al., 1981) obtained by incubating samples at the surface, subsurface, and the SCM for 4 h in a photosynthetron (Xie et al., 2015). These measurements were spectrally corrected and then extrapolated to derive dawn-to-dusk rates of NPP (Kyewalyanga et al., 1997). A separate data set from the South China Sea revealed that dawn-to-dusk rates derived from P-E relationships matched closely with

the 24 h rates, in particular within the lower half of the euphotic zone (see Supplementary Information for the procedure).

(b) During the ONDEQUE cruise, NPP estimates were based on 24 h incubations undertaken in-situ during the day (10–16 h), and on deck in darkened incubators during the night (Barber et al., 2001; Marra et al., 2014).

(c) During the ASN project, NPP rates were measured using ^{14}C labeled $NaHCO_3$ in samples incubated for 24 h under simulated in-situ conditions in on-deck incubators placed in full sunlight and temperature controlled with continuously flowing seawater (Knap 1996).

(d) During the EqPac cruises, primary production was measured in 24 h in-situ incubation experiments using the method described in (b) above.

(e) The NPP values in the NABE project were based on 24 h incubations and similar to (b). In-situ incubations typically extended for about 14 h during the day and the remaining 10 h at dusk were undertaken in the dark in on-deck temperature-controlled incubators.

(f) At HOT, all incubations for NPP from 1990 through mid-2000 were conducted in-situ, in samples drawn from 20 m to 30 m intervals from 0 m to 175 m. Incubations were undertaken from dawn to dusk (10–16 h) in-situ using a free-drifting array. Starting in October 2000, NPP was measured only in samples from the upper six depths. Estimates for the two lower depths (150 m and 175 m) were based on the monthly climatology. Thus, the values of Z_c derived here are based on actual NPP profiles up to 150 m and 175 m from 1998-2000 and a statistical average NPP at 150 and 175 m for 2000–2016. The incubation protocol at BATS is similar to HOT except that the samples were restricted from 0 m to 125 m during 1992–2000.

The value of Z_c for each station was estimated based on the intercept of the linear regression between NPP and depth outside the "well-lit" portion of the profile, usually three or four points, an approach consistent with that in Marra et al. (2014) as the attenuation coefficient does not vary much near the bottom of the euphotic zone. The instantaneous irradiance at Z_c ($I_c(Z_c,t)$) was calculated by integrating $E_d(\lambda,Z_c,t)$ (mol quanta m^{-2} s^{-1} nm^{-1}) from 400 to 700 nm for each profile from these measurements. We then calculated the average ratio of $I_c(Z_c,t)$ to instantaneous irradiance at the surface (PAR(0,t), USR(0,t) and $E_d(490,0,t)$, respectively) for each cruise. Here, the difference between PAR just above the sea surface (PAR(0^+)) and just beneath the surface (PAR(0^-)) is omitted because this difference is just a few percent (see (C. D. Mobley and Boss 2012)), which is small compared to the uncertainties associated with the measurements of PAR(z) or $E_d(\lambda,z)$ or NPP(z).

2.4. Solar Radiation Corresponding to Daily Primary Production

PAR (and USR) changes diurnally, but we assumed that the vertical attenuation remain the same during the day, so that this ratio of $I_c(Z_c,t)$/PAR(0,t) is equivalent to the ratio of $I_c(Z_c$,Daily)/PAR(0,Daily) (see Table 2b). Here, PAR(0,Daily) and USR(0,Daily) represent daily integrated PAR and USR, respectively. A stable value for these ratios is indicative of a link between biological and optical determined euphotic zone. For cruises with measured PAR(0,Daily), we further get $I_c(Z_c$,Daily) as the product of PAR(0,Daily) and $I_c(Z_c,t)$/PAR(0,t). For stations where there were no measured PAR(0,Daily) (CHOICE-C and ASN cruises), the PAR(0,Daily) products from Moderate Resolution Imaging Spectroradiometer (MODIS, https://oceancolor.gsfc.nasa.gov/l3/) were used. Hereinafter for simplicity, I_c, PAR(0), and USR(0) will be referred to $I_c(Z_c$,Daily), PAR(0,Daily), and USR(0,Daily), respectively, unless where its meaning is required to be spelled out with more details.

3. Results

3.1. Characteristics of I_c

Banse (2004) argued that the euphotic depth should be based on I_c–the intensity of solar radiation, rather than $Z_{1\%}^{PAR}$–a measure of relative intensity. A survey of growth-irradiance parameters of laboratory cultures of marine phytoplankton revealed that I_c can vary widely from 0.1 to 0.8 mol quanta m^{-2} d^{-1} (Langdon, 1988). In benthic communities (macroalgae, seagrass, and microphytobentos), Gattuso et al. (2006) found that I_c varied between 0.24 and 4.4 mol quanta m^{-2} d^{-1} and in the west North Atlantic in summer, Marra et al. (2014) observed that I_c can vary between 0.1 and 0.2 mol quanta m^{-2} d^{-1}. Taken together these

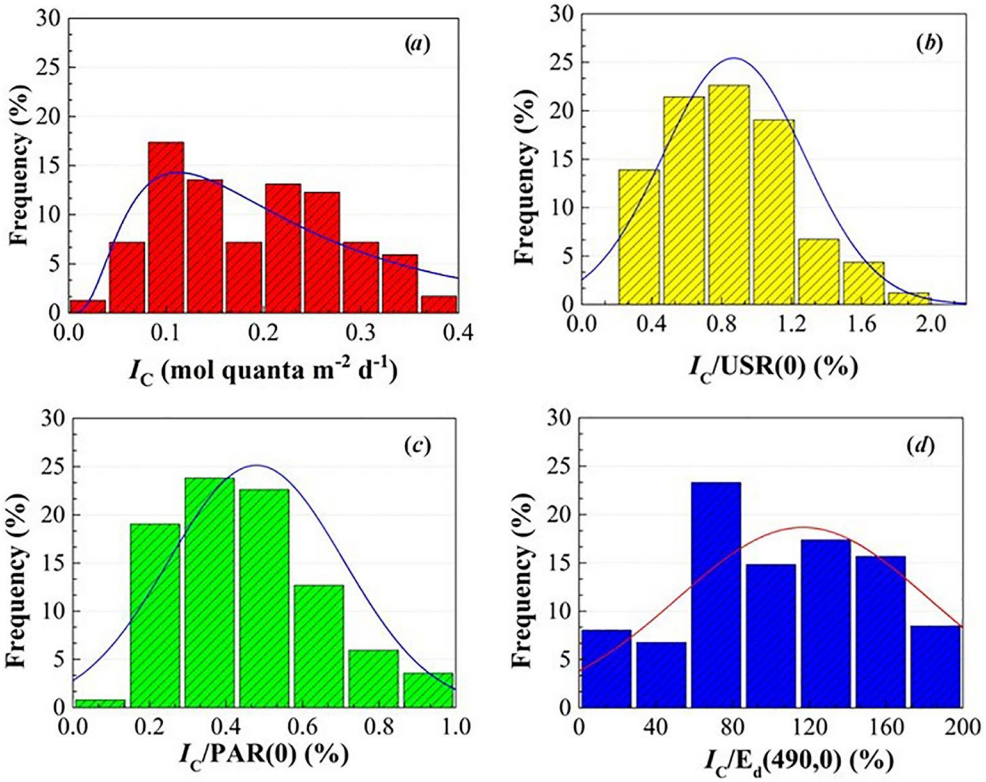

Figure 3. Histograms of (a) I_c, (b) I_c/USR(0), (c) I_c/PAR(0), and (d) $I_c/E_d(490,0)$ from measurements of the seven cruises. The solid curve in each plot represents expected normal distribution from the observed data.

studies suggest that I_c is highly variable and this is consistent with the wide range (~0.03–0.77 mol quanta m^{-2} d^{-1}) of I_c values obtained in this study (see Table 2a and Figure 3a). Figure 3a shows that there is no clear pattern of I_c variability except that >80% vary over a range of 0.07–0.33 mol quanta m^{-2} d^{-1} (CV = 61.4%). Such a wide range of values preclude the use of a constant I_c value as a measure or criterion to determine the base of euphotic zone.

Despite its variability, what is evident in our data set is that I_c values show a dependency on solar radiation at the sea surface. The coefficient of determination (r^2) between I_c and USR(0) is 0.59 (Figure 4a), 0.53 between I_c and PAR(0) (Figure 4b), and 0.44 (Figure 4c) between I_c and E_d (490,0). The slightly stronger correlation for USR is to be expected because radiation in the oceans at Z_c is dominated by wavelengths in the blue-green portion of the visible spectrum (Lee et al., 2014; Lin et al., 2016; Nielsen, 1952), where PAR(0) include photons in the red that cannot reach a depth of Z_c, while E_d (490,0) accounts for solar radiation simply at one wavelength.

3.2. Characteristics of I_c/PAR(0), $I_c/E_d(490,0)$, and I_c/USR(0)

Since I_c varies widely, we analyzed the ratio of I_c to PAR(0), USR(0), and $E_d(490,0)$, respectively following earlier studies (Marra et al., 2014). We note that although I_c varies over a wide range (a factor of five or more, 0.23 ± 0.14 mol quanta m^{-2} d^{-1}), the ratios of I_c to PAR(0), USR(0), and $E_d(490,0)$ are more stable (see Figures 3 and 4). On average, I_c/USR(0) is 0.87% (±0.40%), I_c/PAR(0) is 0.48% (±0.23%), and $I_c/E_d(490,0)$ is 125.3% (±59.0%). These results also indicate that, because of the availability of blue-green light at depth (Lee et al., 2014; Letelier et al., 2017), I_c is significantly greater than $E_d(490,Z_c)$ and can also be larger than $E_d(490,0)$. Detailed ratios of I_c/USR(0) and I_c/PAR(0) for the seven datasets are presented in Table 2b.

Further, following Marra et al. (2014), the ratio of $E_d(490,Z_c)$ to $E_d(490,0)$ was calculated, and it averaged 1.50% ± 0.67% (also see Table 2b), which was also more stable than I_c itself. These results suggest that depths

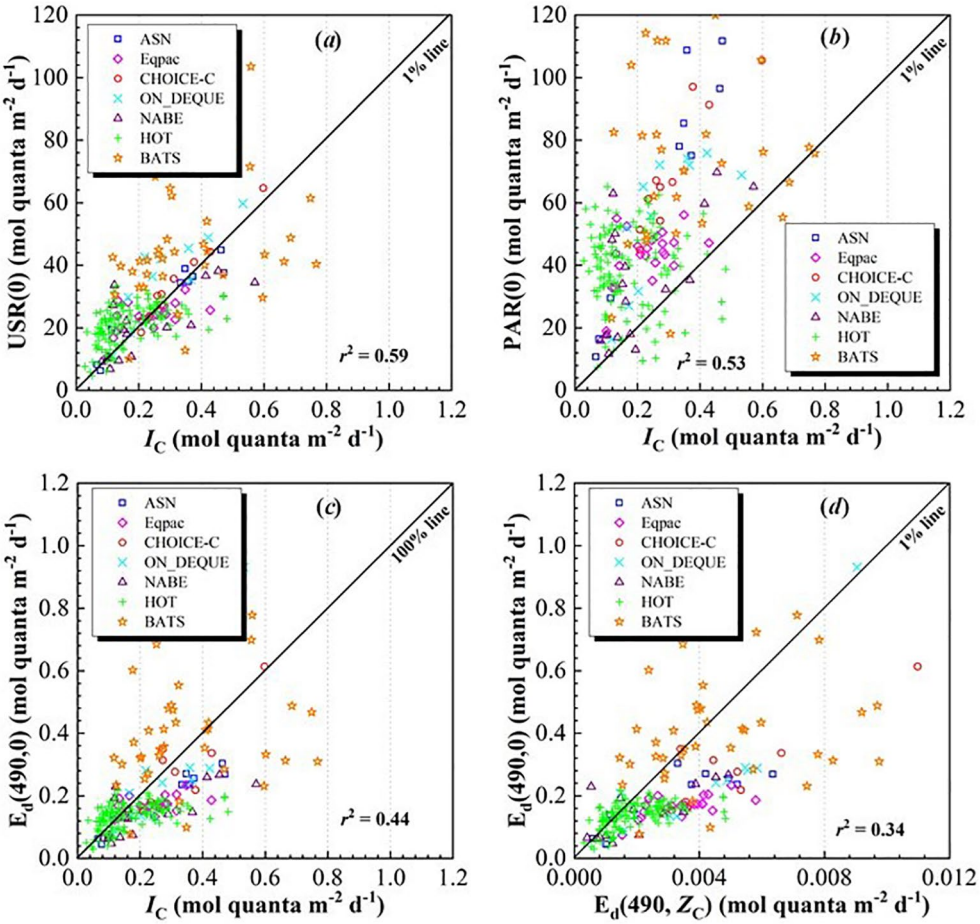

Figure 4. Scatterplots show relationships between I_c and (a) USR(0), (b) PAR(0), and (c) E_d (490,0); (d) relationship between E_d (490,Z_c) and E_d (490,0) using data from the seven cruises.

corresponding to 0.9% USR(0) ($Z_{0.9\%}^{USR}$), 0.5% PAR(0) ($Z_{0.5\%}^{PAR}$) or 1.5% E_d(490,0) ($Z_{1.5\%}^{490}$) match well with Z_c, that is, the biologically determined euphotic zone depth.

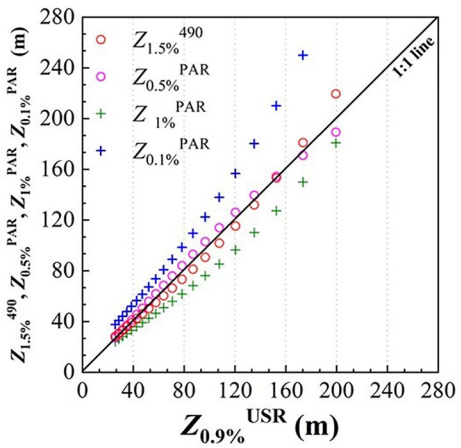

Figure 5. A scatterplot shows relationships between $Z_{0.5\%}^{PAR}$, $Z_{1.5\%}^{490}$, and $Z_{0.9\%}^{USR}$, respectively; also included are $Z_{1\%}^{PAR}$ and $Z_{0.1\%}^{PAR}$, with data from simulations.

3.3. The Consistency Among $Z_{0.9\%}^{USR}$, $Z_{0.5\%}^{PAR}$, and $Z_{1.5\%}^{490}$

The results presented above beg the question, are $Z_{0.9\%}^{USR}$, $Z_{0.5\%}^{PAR}$, and $Z_{1.5\%}^{490}$ consistent with each other? To answer this question, simulations were carried out for waters with absorption (a(490)) coefficients ranging from 0.016 to 0.1 m^{-1} and backscattering coefficients (b_b(490)) from 0.0020 to 0.012 m^{-1}, all at 490 nm and a range covers most oceanic waters. When the values of a(490) and b_b(490) are known, $Z_{0.5\%}^{PAR}$ can be calculated following Lee et al. (2007). Also, with known a(490) and b_b(490) values, the attenuation coefficient of K_d(490) and $Z_{1.5\%}^{490}$ can be calculated following Lee et al., (2013), while $Z_{0.9\%}^{USR}$ be calculated following Lin et al. (2016). Figure 5 shows scatterplots of $Z_{0.5\%}^{PAR}$ and $Z_{1.5\%}^{490}$ against $Z_{0.9\%}^{USR}$ for $Z_{0.9\%}^{USR}$ in a range of 26–200 m, where the slopes are 0.98 ($r^2 > 0.99$, $p < 0.001$). The average ratio of $Z_{0.5\%}^{PAR}$ to $Z_{0.9\%}^{USR}$ is 1.0, while it is 1.05 for $Z_{1.5\%}^{490}$ to $Z_{0.9\%}^{USR}$. These results indicate highly consistent determinations of the euphotic-zone depth from the three different optical properties for the wide range of water properties. The slight (~5.0%) variation is a result of the model simplifications, which is significantly

smaller than the variations observed from field measurements. For comparison, Figure 5 also included scatterplots of $Z_{1\%}^{PAR}$ and $Z_{0.1\%}^{PAR}$ (also following the model of Lee et al., (2007)), where $Z_{1\%}^{PAR}$ is found shallower by 16.4%, while $Z_{0.1\%}^{PAR}$ is deeper by 33.8%, compared to $Z_{0.9\%}^{USR}$. In addition, it is found that on average $Z_{0.1\%}^{PAR}$ is 16.3% deeper than $Z_{1\%}^{490}$. These results differ from those of Laws et al., (2014) who found that for waters of HOT 0.11% surface PAR is equivalent to 1% surface blue light at 475 nm. This discrepancy is addressed in Section 4.4.

4. Discussion

4.1. I_c versus Light Depth for the Determination of Z_{eu}

The results presented above strengthen the view that I_c is not a stable metric for the determination of the euphotic zone as was pointed by Laws et al. (2014) and Marra et al. (2014). It is beyond the scope of our study to probe why I_c varies so widely, but a few clues can be found in Geider et al. (1986) who noted that I_c is determined when the absorbed light meets the requirement of minimum metabolic cost, and this requirement can fluctuate with seawater temperature. Geider et al. (1986) also suggested that the variability of I_c most likely represents a photoacclimation process, which is probably phytoplankton species dependent. Separately, the Chl:carbon ratio also changes under different light conditions. Eppley and Renger (1988), for instance, found that the Chl:carbon ratio at a depth below $Z_{1\%}^{PAR}$ could vary by a factor of 2 within two weeks. These observations again are not supportive of the requirement of a "constant" I_c for determining the euphotic depth.

In addition to its dependence on the radiation at surface, latitude, season, phytoplankton species composition, and the optical properties of water, the datasets obtained here from very different water types show no relationship between I_c and Z_c ($r^2 = 0.05$, $p < 0.05$). On the other hand, as presented earlier, Z_c is highly related to various light threshold depths, such as $Z_{0.9\%}^{USR}$ or $Z_{0.5\%}^{PAR}$ or $Z_{1.5\%}^{490}$. Further, while I_c may change appreciably from day-to-day, the value of $Z_{0.9\%}^{USR}$ (or $Z_{0.5\%}^{PAR}$, $Z_{1.5\%}^{490}$) represents a water property that is relatively constant over short-term periods as bio-optical properties of oceanic waters generally do not change rapidly. Thus, these depths can be reasonable measures of the euphotic depth over a short period.

4.2. The Uncertainties of Z_c and I_c

There is a long-standing debate on whether the ^{14}C method can accurately measure marine primary production. If the ^{12}C-to-^{14}C ratio is assumed to be constant during both photosynthesis and respiration, accurate estimates of NPP are possible, but in reality this assumption is usually not true (Williams & Lefèvre, 2008). We may carefully assume that the ^{12}C-to-^{14}C ratios are approximately the same between the respired carbon that escapes from the cells and the photosynthetically fixed carbon at the sampling depths apparently above the Z_c because the recently fixed carbon is respired (Pei & Laws, 2013).

In this study, the Z_c was in essence estimated following the method in Marra et al. (2014), which is the intercept of the linear regression between NPP versus depth. Due to the limited number of sampling points at deeper depths in the profiles of NPP, the choice of points (3 or 4 lowest depths as suggested) is important, which could lead to 2%–10% difference of Z_c. Additional uncertainties in Z_c could result from types of on-deck incubators, length of incubations, incubator water temperatures that generally rely on circulating sea surface water for samples from depth. A more detailed discussion regarding the impact of incubation lengths, such as dawn-to-dusk (12 h) and dawn-to-dawn (24 h), on Z_c estimates are included the Supporting Information. Even with these various sources of uncertainties, however, we do obtain quite stable relationships between Z_c and $Z_{0.9\%}^{USR}$, or $Z_{0.5\%}^{PAR}$, or $Z_{1.5\%}^{490}$.

We also recognize that at certain locations additional uncertainties in Z_c determinations can result from non-photosynthetic dark uptake of ^{14}C (Graham et al., 2018). The dark-bottle incubation of the ^{14}C method is used to measure the non-photosynthetic carbon fixation (e.g., chemolithoautotrophy and anaplerosis) which is removed in the NPP calculation. The artificial dark environment in the dark bottles could enhance the chemolithoautotrophy, thereby underestimating NPP by an unknown percentage, and the anaplerotic carbon uptake may also be different in between the light and dark bottles. However, the light intensity around the Z_c might be too low to affect the chemolithoautotrophy and anaplerosis, therefore dark carbon

Table 3
Mean Slope Between the Optical Depths and Z_c From the Type II Pearson's Major Axis Regression Through the Match up Points, as well as Its 95% Confidence Intervals and Standard Error

Depth	Slope	Lower bound	Upper bound	Standard error of Slope
$Z_{1\%}^{PAR}$	0.85	0.84	0.86	0.06
$Z_{1\%}^{490}$	1.08	1.06	1.09	0.08
$Z_{0.1\%}^{PAR}$	1.28	1.26	1.29	0.10
$Z_{0.5\%}^{PAR}$	0.94	0.93	0.97	0.07
$Z_{0.9\%}^{USR}$	0.96	0.94	0.97	0.07
$Z_{1.5\%}^{490}$	0.97	0.96	0.98	0.07

*The line of fit forced through the origin.

fixation equals to non-photosynthetic carbon fixation. This is important, as (Laws et al., 2014) showed that Z_c in the North Pacific gyre could be overestimated by 12% and the I_c could be underestimated by 50% by ignoring the non-photosynthetic carbon fixation. For the purpose of this study, non-photosynthetic carbon fixation was accounted for in the NPP calculation for all stations.

In addition to the influence from Z_c, the main uncertainties of estimated I_c also come from the $E_d(\lambda,z)$ profiles, which are based on the average of the three profiles at each station. Statistics show that with a specific station, the difference of each $E_d(\lambda,z)$ profile varies from 3% to 10%. According to the traditional method to calculate $E_d(\lambda,0)$ (Prosoft® 7.7.10), the uncertainty in the estimated $E_d(\lambda,0)$ is found generally within ~6%. While the above mentioned uncertainties are unavoidable in field oceanic measurements, the data from a wide range of waters do emphasize that the ratios of I_c/PAR(0), I_c/USR(0), $I_c/E_d(490,0)$ are more stable as compared to I_c itself.

4.3. Z_c or Z_{max} versus $Z_{1\%}^{PAR}$, $Z_{1\%}^{490}$, $Z_{0.1\%}^{PAR}$

Since Z_c is the biologically derived base of the euphotic zone and the gold standard of its measure, it is always of great interest to see how Z_c varies with respect to other optically based measurements of the euphotic zone (Table 2a), such as $Z_{1\%}^{PAR}$, $Z_{1\%}^{490}$ (the 1% depth of irradiance at 490 nm) and $Z_{0.1\%}^{PAR}$. For all measurements analyzed here (N = 234, Tables 2 and 3), $Z_{1\%}^{PAR}$ (95 ± 24 m) is on average 14.1% shallower than the Z_c ($Z_{1\%}^{PAR} = 0.85 \times Z_c$, $r^2 = 0.83$, $p < 0.001$), supporting previously reported observations that euphotic zone defined by $Z_{1\%}^{PAR}$ is shallower than the compensation depth (Letelier et al., 2004; Lorenzen, 1976). Our results show that I_c/PAR(0) is 0.48% on average, which also suggests that $Z_{0.1\%}^{PAR}$ (138 ± 33 m) will be a significant overestimate (~32.7%) of the euphotic zone depth (Figure 6b and Table 3, $Z_{0.1\%}^{PAR} = 1.28 \times Z_c$, $r^2 = 0.84$, $p < 0.001$).

Recognizing the shortcoming of using $Z_{1\%}^{PAR}$ or $Z_{0.1\%}^{PAR}$ as a measure of the euphotic zone, Marra et al. (2014) and Laws et al. (2014) suggested the use of $Z_{1\%}^{490}$ or $Z_{1\%}^{475}$ as the base of the euphotic zone. However, our analysis indicates that, globally (at least for data in this study), the euphotic zone based on $Z_{1\%}^{490}$ (120 ± 31 m) is ~9.3% deeper than Z_c ($Z_{1\%}^{490} = 1.08 \times Z_c$, $r^2 = 0.83$, $p < 0.001$) (Table 3 and Figure 6b).

In open ocean environments, it is common to observe the presence of the SCM, which is vital for both the food web, carbon cycling and carbon export in oligotrophic waters (Ardyna et al., 2013; Cullen 1982;

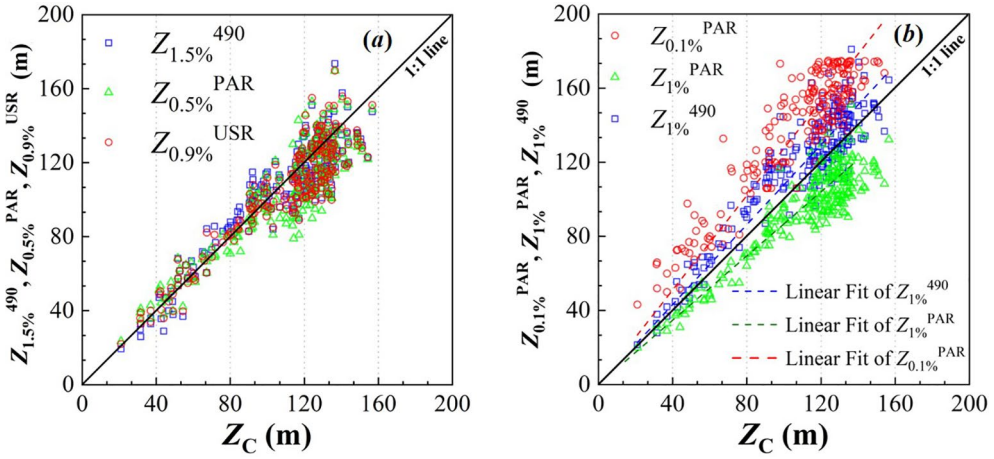

Figure 6. Scatterplots depict relationships between (a) Z_c and $Z_{0.9\%}^{USR}$, $Z_{0.5\%}^{PAR}$, and $Z_{1.5\%}^{490}$; (b) Z_c and $Z_{1\%}^{PAR}$, $Z_{0.1\%}^{PAR}$, and $Z_{1\%}^{490}$.

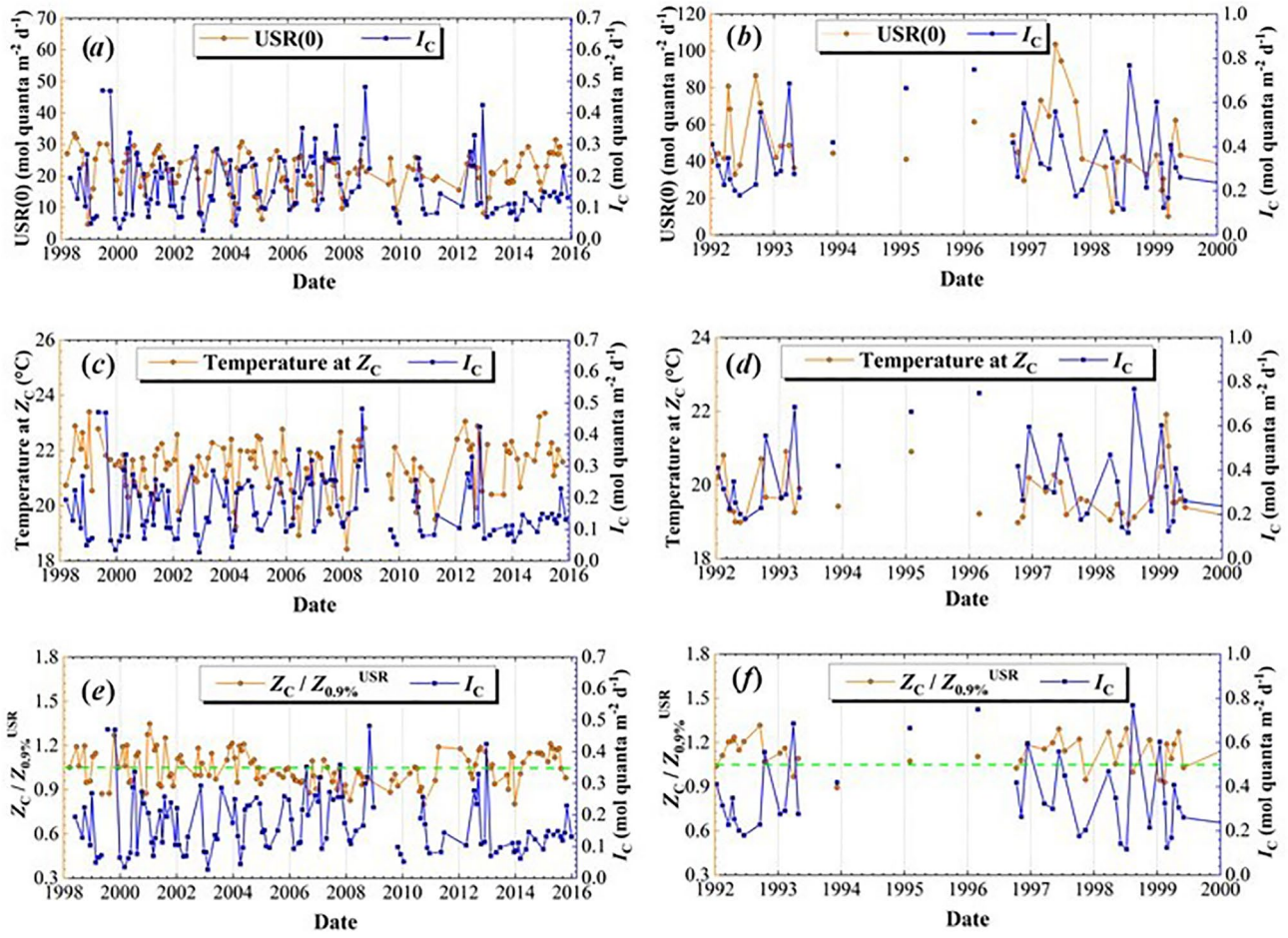

Figure 7. The time-series of the seasonal variation of I_c with (a) USR(0) at HOT station, (b) USR(0) at BATS station, (c) temperature at Z_c in HOT station, (d) temperature at Z_c at BATS station, (e) the ratio of Z_c to $Z_{0.9\%}^{USR}$ at HOT station, and (f) the ratio of Z_c to $Z_{0.9\%}^{USR}$ at BATS station. The green dashed line in (e) and (f) represents the average value of $Z_c/Z_{0.9\%}^{USR}$.

Cullen 2015; Steele & Yentsch, 1960). Thus, it is always worthy to know the relationship between the Z_{max}–the depth of subsurface maximum chlorophyll concentration in the water column–and the light depths. Since the formation of SCMs (under stable conditions) is driven by interactions of light and nutrients (Cullen 2015), it is expected that Z_{max} should be shallower than Z_c. However, our data set (Table 2a) shows that many stations (~36% of our data set) having $Z_{1\%}^{PAR}$ shallower than (by ~8.8% on average) or just at Z_{max} (within 2 m). Since Z_c is the biological base of the euphotic zone and Z_c is always deeper than Z_{max}, these observations again strengthen the notion that $Z_{1\%}^{PAR}$ is too shallow to be representative of the biological euphotic zone. On the other hand, the $Z_{0.9\%}^{USR}$ is on average 35.3%, and always (~94%), deeper than Z_{max}, which indicates that there is adequate light for photosynthesis to take place at the depth of Z_{max} to allow the formation of the SCMs when $Z_{0.9\%}^{USR}$ is used to define the bottom of the euphotic zone.

4.4. Time-Series of HOT and BATS Stations

The time series data from HOT (Figure 7a) and BATS (Figure 7b) allow us to further examine the seasonal variation of I_c and its relation to light intensity at the surface. At HOT station (year 1998–2016), the average I_c is 0.17 ± 0.10 mol quanta m^{-2} d^{-1}, corresponding to 0.81% of USR(0), or 0.44% of PAR(0); while at BATS (year 1992–2000) the average I_c is 0.36 ± 0.18 mol quanta m^{-2} d^{-1}, corresponding to 0.85% of USR(0), or 0.49% of PAR(0). These results again show that I_c is highly variable (with the CV of 56.4% for HOT and 49.8% BATS). However, the influence of temperature at Z_c on the I_c (see Figure 7c for HOT and Figure 7d

for BATS) is limited. The ranges of temperature at Z_c are only ± 1.0°C or so, which is not large enough (especially since they are all relatively "warm" temperatures) to drive much Z_c or I_c variability. Furthermore, the ratio of Z_c to $Z_{0.9\%}{}^{USR}$, or Z_c to $Z_{0.5\%}{}^{PAR}$, is close to 1.0 with a more stable pattern (the CV value is 10.5% for HOT and 11.2% for BATS), despite the fact that Z_c at HOT varied from 100 to 157 m, and 90–135 m at BATS (see Table 2). These results again suggest that $Z_{0.9\%}{}^{USR}$ or $Z_{0.5\%}{}^{PAR}$ maintains a high consistency with Z_c on a long-term scale.

The above results are somewhat different from those reported in Laws et al. (2014), who also estimated I_c and Z_c of HOT using data measured from January 1989 to June 1990 (a total of 16 profiles). Average Z_c reported by them is 155 m, which is deeper by 20 m (12.9%), although both studies used NPP = 0 as the criterion to define the base of the "biological" euphotic zone (Z_c). Consequently, their I_c value is lower. This difference arises from data processing methods that relate NPP with depth. In Laws et al. (2014), it was assumed that in the light-limiting region of the euphotic zone, (1) the photosynthetic rates are proportional to irradiance, and (2) irradiance is linearly related to the logarithm of depth, thus Z_c was determined via a linear regression between NPP and the logarithm of depth (see Figures 1 and 3 in Laws et al. (2014)). Laws et al. (2014) reported that Z_c is 0.11% of PAR(0) or 1% of surface E_d(475). However, the 0.11% depth of PAR(0) in general is much deeper than the 1% depth of surface E_d(475) for oceanic waters (see Figure 6). More specifically, for waters with chlorophyll concentration as 0.1 mg m^{-3} (a value similar to waters at HOT) and based on the "Case 1" bio-optical model (Morel, 2001), the 0.11% depth of PAR(0) is around 135 m simulated from Hydrolight-Ecolight model (version5, Sequoia Scientific) (Mobley and Sundman 2013), but the 1% depth of surface E_d(475) is ∼116 m, that is, the 0.11% of PAR(0) depth is significantly deeper (∼20 m) than the depth of 1% surface E_d(475). This deeper depth of 0.11% PAR(0) compared to 1% E_d(475,0) is consistent with that shown in Figure 6.

In this study, we followed the method in Marra et al. (2014) where NPP near the bottom of the euphotic zone is assumed linearly related to depth. As a result, an average Z_c is found ∼130 m for HOT and ∼115 m for BAT. Further, at BATS, the average I_c is 0.36 ± 0.18 mol quanta m^{-2} d^{-1}, a value higher than the 0.18 ± 0.09 mo quanta m^{-2} d^{-1} reported in Marra et al. (2014) for western North Atlantic, but significantly greater than the 0.054 mol quanta m^{-2} d^{-1} in the Pacific presented in Laws et al. (2014).

4.5. Influence on IPP Estimation

It is now quite clear that euphotic depth based on 1% surface PAR ($Z_{1\%}{}^{PAR}$) is significantly shallower than the biological euphotic zone. Such an underestimation will not only suggest a questionable lower base for the estimation of carbon export (Ducklow et al., 2001; Siegel et al., 2014), but also impact the estimation of water column depth-integrated primary production in low and mid-latitude waters (IPP, mg C m^{-2} d^{-1}) based on models (Behrenfeld & Falkowski, 1997; Cullen et al. 2012; Platt & Sathyendranath, 1993). As a general evaluation of this impact, we carried out a comparison between the integrated primary production down to $Z_{1\%}{}^{PAR}$ (IPP_$Z_{1\%}{}^{PAR}$), $Z_{0.5\%}{}^{PAR}$ (IPP_$Z_{0.5\%}{}^{PAR}$), $Z_{0.9\%}{}^{USR}$ (IPP_$Z_{0.9\%}{}^{USR}$) and to $Z_{1.5\%}{}^{490}$ (IPP_$Z_{1.5\%}{}^{490}$), respectively, and the integrated primary production down to Z_c (IPP_Z_c) at HOT. The mean difference between IPP_ $Z_{1\%}{}^{PAR}$, IPP_ $Z_{0.5\%}{}^{PAR}$, IPP_$Z_{0.9\%}{}^{USR}$ and IPP_ $Z_{1.5\%}{}^{490}$ and the IPP_Z_c is −4.5%, −0.9%, −0.9%, and −0.7%, respectively. Meanwhile, the mean difference between the integrated chlorophyll concentration down to $Z_{1\%}{}^{PAR}$, $Z_{0.5\%}{}^{PAR}$, $Z_{0.9\%}{}^{USR}$ and to $Z_{1.5\%}{}^{490}$ with the integrated chlorophyll concentration down to Z_c is −17.9%, 5.6%, −5.1%, and −4.1%. These results indicate that the conventional IPP_$Z_{1\%}{}^{PAR}$ could result in an average 4.5% and 18% underestimation of water-column integrated primary production and integrated chlorophyll concentration, in part because $Z_{1\%}{}^{PAR}$ could be shallower than Z_{max}, at least in our data set. It appears that the impact of selecting Z_{eu} on IPP is small, this is because that the light intensity is much stronger near the surface, where most of photosynthesis happens. But note that, the IPP within the upper mixed layer does not contribute much to carbon export, whereas the photosynthesis from the mixed-layer depth to the base of the euphotic zone play a much bigger role in carbon export (Ducklow et al., 2001; Siegel et al., 2014), thus the impact of selecting a more appropriate Z_{eu} is much more significant for carbon export than its perceived impact on IPP.

5. Conclusions

Based on a comparison of Z_c with the profiles of spectral light intensity obtained from a wide range of low and mid-latitude open ocean waters, it is found that I_c is highly variable, which reinforces the notion that there is no common I_c value to define the base of the euphotic zone. On the other hand, the ratios of I_c/USR(0), I_c/PAR(0) and $E_d(490,Z_c)/E_d(490,0)$, despite not being constant either, show a clear mode and a narrower range compared to the variation of I_c. Furthermore, at least for waters of this study (no high-latitude measurements), Z_c approximates well the depth where the ratios of USR(Z_c)/USR(0) is ∼0.9%, PAR(Z_c)/PAR(0) is ∼0.5%, or $E_d(490,Z_c)/E_d(490,0)$ is ∼1.5%. Since it is much easier to measure the profile of spectral irradiance, the use of $Z_{0.9\%}^{\mathrm{USR}}$ or $Z_{0.5\%}^{\mathrm{PAR}}$ or $Z_{1.5\%}^{490}$ as a measure of the euphotic zone can thus help reconcile discrepancies between the biological and optical "euphotic zone," at least for low-to mid-latitude oceanic waters. Further, the data and analysis reinforce the notion that $Z_{1\%}^{\mathrm{PAR}}$ is too shallow to represent the euphotic zone. Since about 40% of surface PAR (in the range of 560–700 nm) hardly penetrates oceanic waters, these results further support the argument that "PAR is not the best optical index on which to base the euphotic zone upon" (Marra et al., 2014) and that the use of $Z_{1\%}^{\mathrm{PAR}}$ as a measure of the depth of the euphotic should be replaced by more appropriate radiometric measurements as proposed here.

Data Availability Statement

The CHOICE-C data set is archived in the NCEI World Ocean Database (https://data.nodc.noaa.gov/cgi-bin/iso?id=gov.noaa.nodc:0211060#), more details please see the Supporting Information.

Acknowledgments
This work was jointly supported by the Chinese Ministry of Science and Technology through the National Key Research and Development Program of China (#2016YFA0601201) and the National Natural Science Foundation of China (#41890803, #41830102). JIG is supported by NASA CMS # 80NSSC20K0014. The ONDEQUE and Arabian Sea Noctiluca (ASN) Projects are funded by the National Science Foundation Division of Ocean Sciences (NSF_OCE) under the grant NSF-OCE-0550725 and NSF-OCE-1121022. The authors appreciate https://www.bco-dmo.org/, as well as the Hawaii Ocean Time-series (HOT) program and the Bermuda Bio-Optics Project (BBOP) for providing datasets. The authors also thank NASA OBPG for providing PAR products from ocean color satellite measurements. Comments and suggestions from three anonymous reviewers are greatly appreciated for improving this manuscript.

References

Ardyna, M., Babin, M., Gosselin, M., Devred, E., Bélanger, S., Matsuoka, A., & Tremblay, J.-É. (2013). Parameterization of vertical chlorophyll a in the Arctic Ocean: Impact of the subsurface chlorophyll maximum on regional, seasonal, and annual primary production estimates. *Biogeosciences*, *10*, 4383–4404. https://doi.org/10.5194/bg-10-4383-2013

Banse, K. (2004). Should we continue to use the 1% light depth convention for estimating the compensation depth of phytoplankton for another 70 years. *Limnology and Oceanography Bulletin*, *13*, 49–52. https://doi.org/10.1002/lob.200413349

Barber, R. T., Marra, J., Bidigare, R. C., Codispoti, L. A., Halpern, D., Johnson, Z., et al. (2001). Primary productivity and its regulation in the Arabian Sea during 1995. *Deep Sea Research Part II: Topical Studies in Oceanography*, *48*, 1127–1172. https://doi.org/10.1016/s0967-0645(00)00134-x

Behrenfeld, M. J., & Falkowski, P. G. (1997). A consumer's guide to phytoplankton primary productivity models. *Limnology & Oceanography*, *42*, 1479–1491. https://doi.org/10.4319/lo.1997.42.7.1479

Cullen, J. J. (1982). The deep chlorophyll maximum: Comparing vertical profiles of chlorophyll a. *Canadian Journal of Fisheries and Aquatic Sciences*, *39*, 791–803. https://doi.org/10.1139/f82-108

Cullen, J. J. (2015). Subsurface chlorophyll maximum layers: Enduring enigma or mystery solved? *Annual Review of Marine Science*, *7*, 207–239. https://doi.org/10.1146/annurev-marine-010213-135111

Cullen, J. J., Davis, R. F., & Huot, Y. (2012). Spectral model of depth-integrated water column photosynthesis and its inhibition by ultraviolet radiation. *Global Biogeochemical Cycles*, *26*, GB1011. https://doi.org/10.1029/2010GB003914

Dubinsky, Z., Falkowski, P. G., & Wyman, K. (1986). Light harvesting and utilization by phytoplankton. *Plant and Cell Physiology*, *27*, 1335–1349. https://doi.org/10.1093/oxfordjournals.pcp.a077232

Ducklow, H., Steinberg, D., & Buesseler, K. (2001). Upper ocean carbon export and the biological pump. *Oceanog*, *14*, 50–58. https://doi.org/10.5670/oceanog.2001.06

Eppley, R. W., & Peterson, B. J. (1979). Particulate organic matter flux and planktonic new production in the deep ocean. *Nature*, *282*, 677–680. https://doi.org/10.1038/282677a0

Eppley, R. W., & Renger, E. H. (1988). Nanomolar increase in surface layer nitrate concentration following a small wind event. *Deep-Sea Research Part A. Oceanographic Research Papers*, *35*, 1119–1125. https://doi.org/10.1016/0198-0149(88)90004-0

Falkowski, P. G. (1994). The role of phytoplankton photosynthesis in global biogeochemical cycles. *Photosynthesis Research*, *39*, 235–258. https://doi.org/10.1007/bf00014586

Gattuso, J.-P., Gentili, B., Duarte, C. M., Kleypas, J. A., Middelburg, J. J., Antoine, D., et al. (2006). Light availability in the coastal ocean: Impact on the distribution of benthic photosynthetic organisms and their contribution to primary production. *Biogeosciences*, *3*, 489–513. https://doi.org/10.5194/bg-3-489-2006

Geider, R., Piatt, T., & Raven, J. (1986). Size dependence of growth and photosynthesis in diatoms: A synthesis. *Marine Ecology Progress Series*, *30*, 93–104. https://doi.org/10.3354/meps030093

Graham, E. D., Heidelberg, J. F., & Tully, B. J. (2018). Potential for primary productivity in a globally-distributed bacterial phototroph. *The ISME Journal*, *12*, 1861–1866. https://doi.org/10.1038/s41396-018-0091-3

Holm-Hansen, O., & Greg Mitchell, B. (1991). Spatial and temporal distribution of phytoplankton and primary production in the western Bransfield Strait region. *Deep-Sea Research Part A. Oceanographic Research Papers*, *38*, 961–980. https://doi.org/10.1016/0198-0149(91)90092-t

Hung, C.-C., Wong, G. T. F., Liu, K.-K., Fuh-Kwo, S., & Gwo-Ching, G. (2000). The effects of light and nitrate levels on the relationship between nitrate reductase activity and 15 NO3 − uptake: Field observations in the East China Sea. *Limnology & Oceanography*, *45*, 836–848. https://doi.org/10.4319/lo.2000.45.4.0836

Kirk, J. T. (1994). *Light and photosynthesis in aquatic ecosystems*. Cambridge university press. https://doi.org/10.1017/cbo9780511623370

Knap, A. H., Michaels, A., Close, A. R., Ducklow, H., & Dickson, A. G. (1996). Protocols for the joint global ocean flux study (JGOFS) core measurements, *19*, Paris, France: UNESCO-IOC.

Kyewalyanga, M., Platt, T., & Sathyendranath, S. (1997). Estimation of the photosynthetic action spectrum: Implication for primary production models. *Marine Ecology Progress Series*, *146*, 207–223. https://doi.org/10.3354/meps146207

Langdon, C. (1988). On the causes of interspecific differences in the growth-irradiance relationship for phytoplankton. II. A general review. *Journal of Plankton Research*, *10*, 1291–1312. https://doi.org/10.1093/plankt/10.6.1291

Laws, E. A., Letelier, R. M., & Karl, D. M. (2014). Estimating the compensation irradiance in the ocean: The importance of accounting for non-photosynthetic uptake of inorganic carbon. *Deep Sea Research Part I: Oceanographic Research Papers*, *93*, 35–40. https://doi.org/10.1016/j.dsr.2014.07.011

Lee, Z., Hu, C., Shang, S., Du, K., Lewis, M., Arnone, R., & Brewin, R. (2013). Penetration of UV-visible solar radiation in the global oceans: Insights from ocean color remote sensing. *Journal of Geophysical Research: Oceans*, *118*, 4241–4255. https://doi.org/10.1002/jgrc.20308

Lee, Z. P., Weidemann, A., Kindle, J., Arnone, R., Carder, K. L., & Davis, C. (2007). Euphotic zone depth: Its derivation and implication to ocean-color remote sensing. *Journal of Geophysical Research: Oceans*, *112*, C03009. https://doi.org/10.1029/2006jc003802

Lee, Z., Shang, S., Du, K., Wei, J., & Arnone, R. (2014). Usable solar radiation and its attenuation in the upper water column. *Journal of Geophysical Research: Oceans*, *119*, 1488–1497. https://doi.org/10.1002/2013jc009507

Letelier, R. M., Karl, D. M., Abbott, M. R., & Bidigare, R. R. (2004). Light driven seasonal patterns of chlorophyll and nitrate in the lower euphotic zone of the North Pacific Subtropical Gyre. *Limnology & Oceanography*, *49*, 508–519. https://doi.org/10.4319/lo.2004.49.2.0508

Letelier, R. M., White, A. E., Bidigare, R. R., Barone, B., Church, M. J., & Karl, D. M. (2017). Light absorption by phytoplankton in the North Pacific Subtropical Gyre. *Limnology & Oceanography*, *62*, 1526–1540. https://doi.org/10.1002/lno.10515

Lin, J., Lee, Z., Ondrusek, M., & Du, K. (2016). Remote sensing of normalized diffuse attenuation coefficient of downwelling irradiance. *Journal of Geophysical Research: Oceans*, *121*, 6717–6730. https://doi.org/10.1002/2016jc011895

Lorenzen, C. (1976). Primary production in the sea. *Ecology of the seas*, 173–185.

Marra, J. F., Lance, V. P., Vaillancourt, R. D., & Hargreaves, B. R. (2014). Resolving the ocean's euphotic zone. *Deep Sea Research Part I: Oceanographic Research Papers*, *83*, 45–50. https://doi.org/10.1016/j.dsr.2013.09.005

Mobley, C. D., & Boss, E. S. (2012). Improved irradiances for use in ocean heating, primary production, and photo-oxidation calculations. *Applied Optics*, *51*, 6549–6560. https://doi.org/10.1364/ao.51.006549

Mobley, C., & Sundman, L. (2013). *HydroLight 5.2 User's Guide*. Bellevue, DC: Sequoia Scientific. In.

Morel, A. (2001). *Bio-optical models*. Academic Press.

Nielsen, S. (1952). The use of radio-active carbon (c14) for measuring organic production in the sea. *ICES Journal of Marine Science*, *18*, 24. https://doi.org/10.1093/icesjms/18.2.117

Nielsen, S., & Hansen, K. V. (1961). Influence of surface illumination on plankton photosynthesis in Danish water (56°N) throughout the year. *Physiologia Plantarum*, *14*, 595–613. https://doi.org/10.1111/j.1399-3054.1961.tb07917.x

Parsons, T., Maita, Y., & Lalli, C. (1984). A manual of chemical and biological methods for seawater analysis. Pergamon, Oxford sized algae and natural seston size fractions. *Marine Ecology Progress Series*, *199*, 43–53.

Parsons, T. R., Takahashi, M., & Hargrave, B. (2013). *Biological oceanographic processes*. Elsevier.

Pei, S., & Laws, E. A. (2013). Does the ^{14}C method estimate net photosynthesis? Implications from batch and continuous culture studies of marine phytoplankton. *Deep Sea Research Part I: Oceanographic Research Papers*, *82*, 1–9. https://doi.org/10.1016/j.dsr.2013.07.011

Platt, T., Gallegos, C., & Harrison, W. G. (1981). Photoinhibition of photosynthesis in natural assemblages of marine phytoplankton. *AGRIS*, *38*, 687–701.

Platt, T., & Sathyendranath, S. (1993). Fundamental issues in measurement of primary production. In W. K. W. Li, & S. Y. Maestrini (Eds.), *Measurement of primary production from the molecular to the global scale* (pp. 3–8). ICES Marine Science Symposium.

Richardson, T. L., & Jackson, G. A. (2007). Small phytoplankton and carbon export from the surface ocean. *Science*, *315*, 838–840. https://doi.org/10.1126/science.1133471

Ryther, J. H. (1955). The ratio of photosynthesis to respiration in marine plankton algae and its effect upon the measurement of productivity. *Deep-Sea Research*, *2*, 134–139. https://doi.org/10.1016/0146-6313(55)90015-0

Ryther, J. H. (1956). Photosynthesis in the ocean as a function of light intensity1. *Limnology & Oceanography*, *1*, 61–70. https://doi.org/10.4319/lo.1956.1.1.0061

Sager, J. C., & McFarlane, J. C. (1997). Radiation. *Plant growth chamber handbook* (pp. 1–29).

Siegel, D. A., Buesseler, K. O., Doney, S. C., Sailley, S. F., Behrenfeld, M. J., & Boyd, P. W. (2014). Global assessment of ocean carbon export by combining satellite observations and food-web models. *Global Biogeochemical Cycles*, *28*, 181–196. https://doi.org/10.1002/2013gb004743

Steele, J. H., & Yentsch, C. S. (1960). The vertical distribution of chlorophyll. *Journal of the Marine Biological Association*, *39*, 217–226. https://doi.org/10.1017/s0025315400013266

Williams, P. J. l. B., & Lefèvre, D. (2008). An assessment of the measurement of phytoplankton respiration rates from dark ^{14}C incubations. *Limnology and Oceanography: Methods*, *6*, 1–11. https://doi.org/10.4319/lom.2008.6.1

Xie, Y., Huang, B., Lin, L., Laws, E. A., Wang, L., Shang, S., et al. (2015). Photosynthetic parameters in the northern South China Sea in relation to phytoplankton community structure. *Journal of Geophysical Research: Oceans*, *120*, 4187–4204. https://doi.org/10.1002/2014jc010415

Zoffoli, M. L., Lee, Z., & Marra, J. F. (2018). Regionalization and dynamic parameterization of quantum yield of photosynthesis to improve the ocean primary production estimates from Remote Sensing. *Frontiers in Marine Science*, *5*, 446. https://doi.org/10.3389/fmars.2018.00446